



OPEN *SAMHD1* dysfunction impairs DNA damage response and increases sensitivity to PARP inhibition in chronic lymphocytic leukemia

Alberto Rodríguez-Sánchez^{1,2}, Miguel Quijada-Álamo^{1,2,3}, Claudia Pérez-Carretero^{1,2}, Ana B. Herrero^{1,4}, Andrés Arroyo-Barea⁵, Julio Dávila-Valls⁶, Araceli Rubio⁷, Alfonso García de Coca⁸, Rocío Benito-Sánchez^{1,2}, Ana E. Rodríguez-Vicente^{1,9}, Jesús María Hernández-Rivas^{1,2,10} & María Hernández-Sánchez^{1,5,10}✉

Chronic lymphocytic leukemia (CLL) is a clinically and genetically heterogeneous disease. Recent next-generation sequencing (NGS) studies have uncovered numerous low-frequency mutated genes in CLL patients, with *SAMHD1* emerging as a candidate driver gene. However, the biological and clinical implications of *SAMHD1* mutations remain unclear. Using CRISPR/Cas9, we generated CLL models to investigate the impact of *SAMHD1* deficiency on pathogenesis and explore therapeutic strategies. Moreover, we performed NGS in treatment-naïve CLL patients to characterize *SAMHD1* mutations and employed RNA-sequencing to evaluate their clinical significance. Our study shows that *SAMHD1* inactivation impairs the DNA damage response by reducing homologous recombination efficiency through BRCA1 and RAD51 dysregulation. Importantly, *SAMHD1* colocalizes with BRCA1 at DNA damage sites in CLL cells. This research also identifies that *SAMHD1*-mutated cells are more sensitive to PARP inhibition. Clinically, *SAMHD1* dysfunction negatively impacts clinical outcome of CLL cases: *SAMHD1* mutations reduce failure-free survival (median 46 vs 57 months, $p = 0.033$), while low *SAMHD1* expression associates with shorter time to first treatment (median 47 vs 77 months; $p = 0.00073$). Overall, this study elucidates that *SAMHD1* dysfunction compromises DNA damage response mechanisms, potentially contributing to unfavorable clinical outcomes in CLL, and proposes PARP-inhibitors as a potential therapeutic approach for *SAMHD1*-mutated CLL cells.

Chronic lymphocytic leukemia (CLL) exhibits both a heterogeneous clinical and biological course, reflecting the complex genetic landscape of the disease^{1,2}. Recent large-scale next generation sequencing (NGS) studies of CLL patients have identified over 200 candidate driver genes, predominantly exhibiting low mutational incidences ($< 5\%$)^{3–5}. Among these, *SAMHD1* has been uncovered as a potential CLL driver. However, the prognostic and biological implications of its alterations are poorly understood.

SAMHD1 is a nuclear triphosphohydrolase which converts all four deoxynucleotide triphosphates (dNTPs) to deoxynucleosides and inorganic triphosphate. By regulating cellular dNTPs levels, *SAMHD1* plays a key role in the maintenance of homeostasis of dNTPs pools and is essential for the preservation of genomic integrity^{6–8}. An imbalance in the dNTPs levels associates with DNA replication stress, reduced genomic stability and impaired DNA breaks repair mechanisms^{9,10}. Apart from its dNTPase function, *SAMHD1* also plays a direct role in DNA double-strand breaks (DSB) repair, promoting DNA end resection to facilitate DNA lesions repair by homologous recombination (HR) through the recruitment of DSB repair machinery¹¹.

¹Centro de Investigación del Cáncer, Universidad de Salamanca, IBSAL, IBMCC, CSIC, Salamanca, Spain. ²Servicio de Hematología, Hospital Universitario de Salamanca, Salamanca, Spain. ³Department of Oncological Sciences, Icahn School of Medicine at Mount Sinai, New York, NY, USA. ⁴Departamento de Medicina, Unidad de Medicina Molecular, Universidad de Salamanca, Salamanca, Spain. ⁵Departamento de Bioquímica y Biología Molecular, Facultad de Farmacia, Universidad Complutense de Madrid, Madrid, Spain. ⁶Servicio de Hematología, Hospital Nuestra Señora de Sonsoles, SACYL, Ávila, Spain. ⁷Servicio de Hematología, Hospital Miguel Servet, SERGAS, Zaragoza, Spain. ⁸Servicio de Hematología, Hospital Clínico, SACYL, Valladolid, Spain. ⁹Departamento de Anatomía e Histología Humanas, Facultad de Medicina, Universidad de Salamanca, Salamanca, Spain. ¹⁰These authors jointly supervised this work: Jesús María Hernández-Rivas and María Hernández-Sánchez. ✉email: mariahs@ucm.es

Germline *SAMHD1* mutations are reported in Aicardi-Goutières syndrome (AGS)^{12,13}. Importantly, clinical observations have involved *SAMHD1* mutations with CLL pathogenesis, as evidenced by an AGS patient with *SAMHD1* mutated but lacking other CLL-related mutations who developed CLL¹⁴. In addition, somatic *SAMHD1* mutations occur in ~2% of newly diagnosed CLL patients⁵ and up to 11% of relapsed or chemotherapy-refractory cases, often as early clonal events^{5,15}. Previous studies have suggested that *SAMHD1* mutations typically lead to significantly reduced mRNA and protein expression¹⁴.

Despite the huge advances in improving CLL genetic characterization, the impact of some recurrently mutated genes such as *SAMHD1* remains insufficiently understood. This study aims to delineate the implications of *SAMHD1* variants in CLL. To elucidate their biological impact, novel isogenic CLL cellular models with loss-of-function mutations in *SAMHD1* were generated using CRISPR/Cas9. Given the known involvement of *SAMHD1* in the DNA damage response (DDR), our results show that *SAMHD1* dysfunction reduces HR efficiency through impaired recruitment of BRCA1 to DNA damage sites, showing a functional interaction between *SAMHD1* and BRCA1. Moreover, we correlated defective DDR with increased sensitivity to olaparib, suggesting potential therapeutic benefits of PARP inhibition in *SAMHD1*-mutated CLL patients. Furthermore, to assess their prognostic significance, we evaluated *SAMHD1* mutational status in a treatment-naïve cohort and analyzed the clinical effects of its dysfunction using genomic and transcriptomic data, revealing an unfavorable clinical outcome. These findings position *SAMHD1* as a critical mediator of DNA repair and genomic stability in CLL, with important implications for both prognosis and targeted therapy.

Results

SAMHD1 deficiency disrupts the DNA damage response by impairing the recruitment of HR marker BRCA1

To investigate the biological implications of *SAMHD1* mutations, we conducted an in-depth analysis using transcriptomic datasets from CLL patients collected in the CLL-map portal³. Through this approach, we identified a comprehensive list of genes whose expression is significantly correlated with *SAMHD1* expression in CLL patients (Supplementary Table 5). Functional annotation of these genes highlighted the DNA damage response as one of the most significantly enriched pathways (Fig. 1A). To gain deeper insights, we generated *SAMHD1*^{KO} cells in PGA1 and MEC1 CLL-derived cell lines following the experimental design shown in Supplementary Fig. 1A. The introduction of truncating mutations in *SAMHD1* gene (Supplementary Fig. 1B) resulted in the absence of protein (Supplementary Fig. 1C).

The role of *SAMHD1* in maintaining genome stability by promoting HR¹¹ prompted us to evaluate the efficiency of the two main mechanisms of DSBs repair: HR and non-homologous end joining (NHEJ). Functional assays in CLL models demonstrated a significantly reduced HR efficiency in *SAMHD1*^{KO} cells compared to *SAMHD1*^{WT} counterparts, ($p < 0.05$) (Fig. 1B). In contrast, *SAMHD1* truncation did not cause significant changes in NHEJ efficiency (Supplementary Fig. 2).

Strikingly, analysis of patients samples from the CLL-map portal revealed a significant positive correlation between *SAMHD1* and *BRCA1* expression ($R = 0.36$, $p < 0.0001$) (Fig. 1C). These findings led us to investigate whether *SAMHD1* directly impacts *BRCA1* recruitment. In response to ionizing radiation (IR), *SAMHD1*^{KO} cells exhibited a statistically significant reduction of *BRCA1 foci* ($p < 0.0001$) (Fig. 1D), indicating defective recruitment of *BRCA1* to DSBs. Importantly, *SAMHD1* colocalized with *BRCA1* at DSBs sites following IR (Fig. 1E), suggesting a cooperation of *SAMHD1* and *BRCA1* in DDR. Furthermore, *SAMHD1* disruption significantly impaired the localization of RAD51 to DSB sites in γ H2AX-positive cells ($p < 0.05$) (Fig. 1F), indicating that *SAMHD1* is essential for the efficient localization of these HR machinery components.

We tested *in vitro* how *SAMHD1*^{KO} cells responded to DSBs. *SAMHD1*^{KO} cells were more sensitive to DNA damage inducers such as IR (Supplementary Fig. 3A) or etoposide, validating this hypersensitivity in MEC1 cells (Supplementary Fig. 3B). Subsequently, we examined the expression levels of key protein kinases involved in the signaling pathways associated with DSB repair. Upon etoposide treatment, *SAMHD1*^{KO} cells exhibited reduced phosphorylation levels of ATM, ATR and CHK1, concomitant with higher CHK2 phosphorylation (Fig. 1G). By contrast, we did not observe changes in expression levels of ATM, ATR, CHK1 and CHK2. Then, we determined cell cycle profile of PGA1 cells 48 h post-IR. As expected, *SAMHD1*^{WT} cells exhibited cell cycle arrest in G2/M phase, indicative of an active repair process in response to DNA damage, whereas *SAMHD1*^{KO} cells overcame this point and showed the same profile that those cells without IR exposure (Supplementary Fig. 3C). A similar cell cycle distribution was observed in MEC1 cells (Supplementary Fig. 3D). In addition, an analysis comparing *SAMHD1*^{KO} to *SAMHD1*^{WT} cells revealed a statistically significant reduction in G2/M arrest in CLL cells with *SAMHD1* dysfunction ($p < 0.001$) (Supplementary Fig. 3E). These findings underscore the impact of *SAMHD1* deficiency on cellular response to DSBs.

SAMHD1^{KO} cells are more sensitive to DNA damage inducers

Considering the potential of defects in DNA damage repair to increase sensitivity to various DNA damage-inducing agents, we tested the impact of *SAMHD1* truncation on the cellular response to the alkylating agent bendamustine and the nucleoside analogue fludarabine. Notably, *SAMHD1*^{KO} cells exhibited higher sensitivity to both drugs approved for CLL therapy (Fig. 2A,B). Remarkably, *SAMHD1*^{KO} cells showed a significant lower fludarabine IC₅₀ compared with *SAMHD1*^{WT} (mean IC₅₀ of *SAMHD1*^{WT}: 9.8 μ M vs *SAMHD1*^{KO}: 2.5 μ M, $p < 0.0001$). This higher sensitivity was also validated in *SAMHD1*^{KO} MEC1 cells, which harbor *TP53* dysfunction (Supplementary Fig. 4A,B). Interestingly, HG3 cells, harboring a truncating mutation in *SAMHD1*, showed the lowest IC₅₀ value for fludarabine (Fig. 2C, Supplementary Table 1). This result supports that *SAMHD1* inactivating mutations enhance sensitivity to fludarabine, which is a *SAMHD1* substrate.

We next demonstrated that fludarabine treatment increases apoptosis and modifies cell cycle profile. Annexin V/PI staining revealed a higher percentage of apoptotic (annexin V+) and late apoptotic *SAMHD1*^{KO}

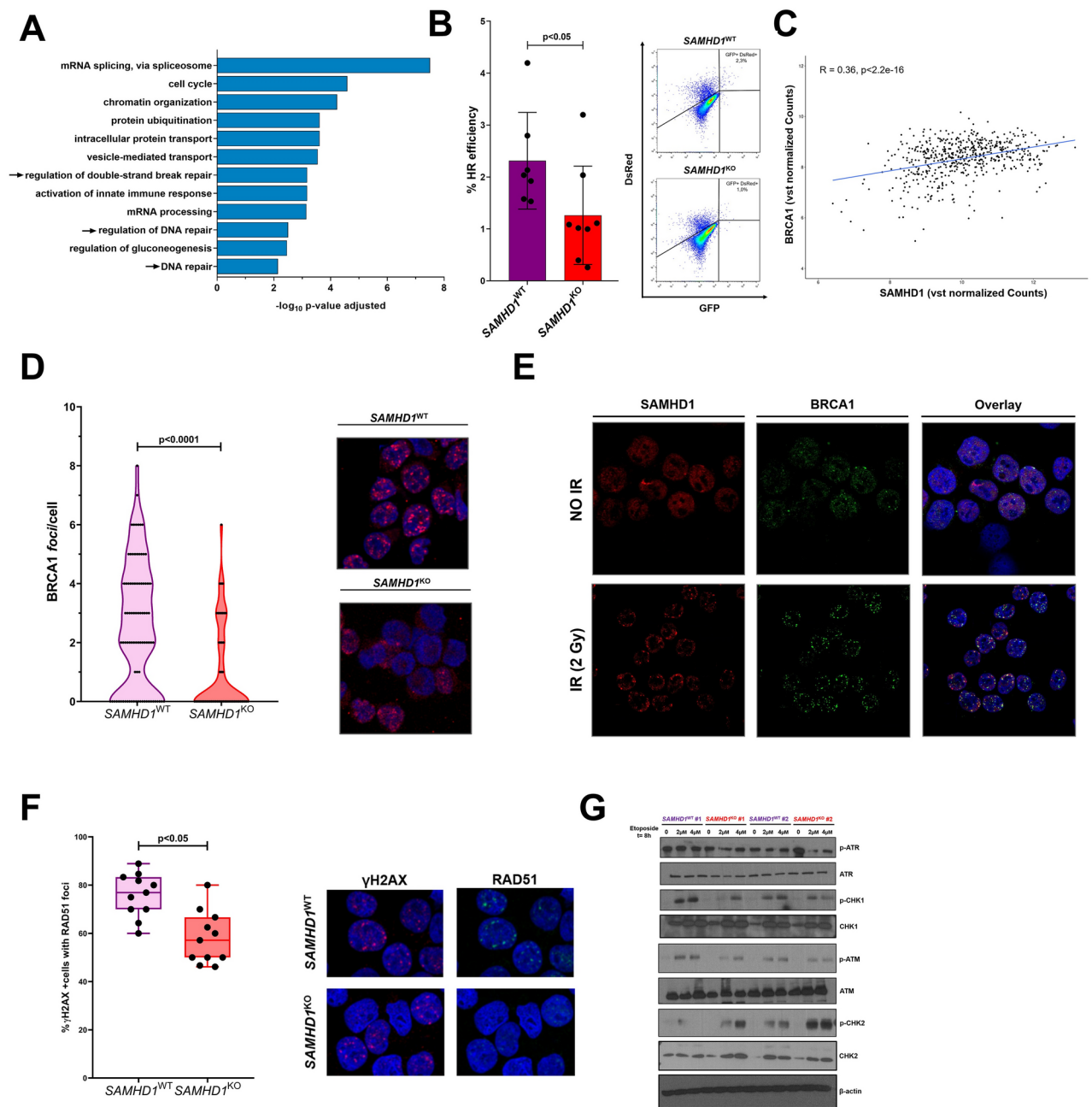


Fig. 1. Biological effects of *SAMHD1* dysfunction in DNA damage response in CLL. **(A)** Plots depicting GO analysis results of the top significantly enriched pathways correlated with *SAMHD1* expression in CLL patients. Arrows emphasize the biological processes related with DNA damage response. **(B)** Left panel: HR efficiency graph for DSB repair in PGA1 cell line using a HR reporter plasmid. HR repair efficiency was calculated as the ratio of GFP + cells to the total number of DsRed + (transfected) cells. Three clones per condition in 3 independent experiments were analyzed. Results are shown as mean \pm SD. Right panel: Representative plots of HR repair in *SAMHD1*^{WT} and *SAMHD1*^{KO} cells. **(C)** Correlation analysis between *BRCA1* and *SAMHD1* mRNA expression normalized with the vst score in CLL patients from the CLL map project. **(D)** Left panel: Quantification of *BRCA1* foci/cell in *SAMHD1*^{WT} and *SAMHD1*^{KO} cells 1-h post-IR. At least fifty cells were counted per experiment in two independent clones per condition. Right panel: Representative images of *BRCA1*-positive cells 1 h after irradiation (2 Gy). **(E)** Representative immunofluorescence images showing the colocalization of *SAMHD1* with *BRCA1* at DNA damage sites following 2 Gy irradiation. Images include untreated control (no irradiation) and irradiated (DNA-damage induced) conditions. **(F)** Left panel: Measurement of *RAD51* foci/cell in γ H2AX positive cells 6 h post-IR. Cells were considered as γ H2AX + when 5 or more foci were formed. At least fifty cells were counted per experiment. Two independent experiments were performed in three biological replicates. Right panel: Representative images of γ H2AX + cells and *RAD51* localization. **(G)** Western blot analyses depicting the expression of the proteins implicated in DNA damage signaling ATM, ATR, Chk1 and Chk2; and their phosphorylated forms. Cells were not treated (0), or treated with 2 or 4 μ M of etoposide for 8 h. Two single-cell clones were analyzed for each condition.

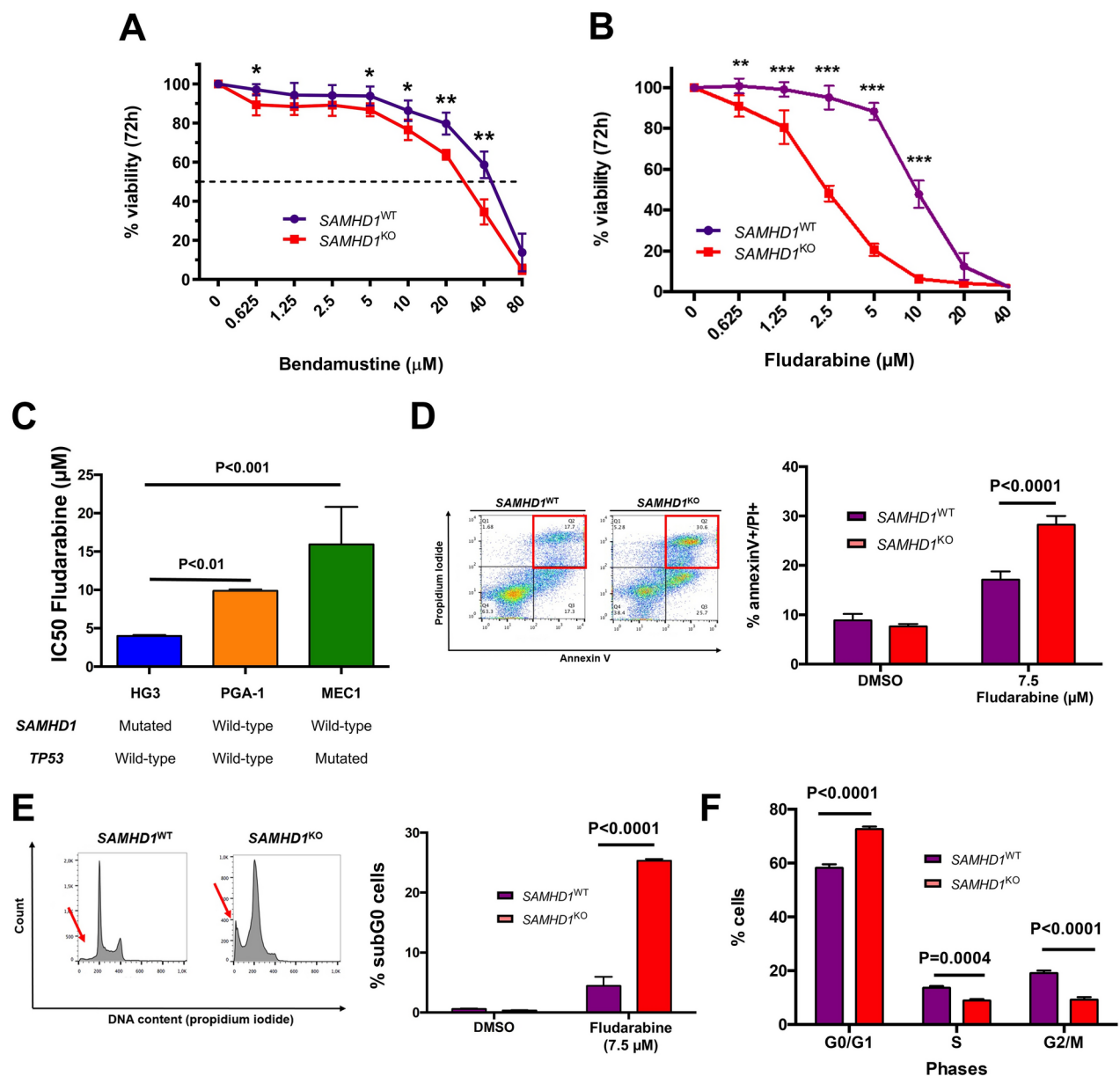


Fig. 2. Impact of SAMHD1 disruption on response to DNA damage inducers. **(A, B)** Dose–response curves of bendamustine **(A)** and fludarabine **(B)** treatment in PGA1 cell line. Cells were treated with escalating doses of bendamustine (0.625–80 μM) or fludarabine (0.625–40 μM) for 72 h. Cell viability was assessed with MTT, and surviving fraction is expressed relative to DMSO control. Dashed line represents the reduction of IC50 value in $\text{SAMHD1}^{\text{KO}}$ cells. Data are represented as mean \pm SD of three independent experiments. **(C)** IC50 value (μM) for fludarabine treatment in 3 CLL cell lines (HG3, PGA-1 and MEC1). Information of SAMHD1 and TP53 status were summarized below the graph. **(D)** Representative annexin V/PI dot-plots (left panel) to determine apoptotic (annexin V+/PI+) cells (right panel) after 7.5 μM fludarabine for 48 h. **(E)** PI staining for determination of subG0 population (left panel) for PGA1 cells, reflecting the increase of apoptotic $\text{SAMHD1}^{\text{KO}}$ cells after fludarabine treatment (right panel). **(F)** Cell cycle profile determined by PI staining after 48 h fludarabine treatment (7.5 μM) in PGA1 cell line. Data are represented as mean \pm SD of three independent experiments.

cells (annexin V + PI+) (Fig. 2D) compared to $\text{SAMHD1}^{\text{WT}}$ cells. Apoptosis enhancement was also confirmed by the higher subG0 percentage in $\text{SAMHD1}^{\text{KO}}$ cells, a characteristic marker of apoptosis (Fig. 2E). In parallel, we identified a higher G1 percentage and a concomitant reduction of cells in G2/M after fludarabine treatment in $\text{SAMHD1}^{\text{KO}}$ cells compared to the WT counterparts (Fig. 2F, Supplementary Fig. 4C).

***SAMHD1*^{KO} cells are more sensitive to PARP inhibition by olaparib**

Considering the reduced HR efficiency in *SAMHD1*^{KO} cells and the well-established association between HR defects and increased sensitivity to poly-ADP-ribose polymerase (PARP) inhibitors³⁵, we hypothesized that PARP inhibition could be an attractive treatment for *SAMHD1*^{KO} cells. First, we observed that *SAMHD1*^{KO} potentiated sensitivity to PARP inhibition with olaparib in PGA1 cells, which show a significant decrease of IC50 value (4.014 vs 8.383 μ M), (Fig. 3A). This hypersensitivity to olaparib was corroborated in MEC1 *SAMHD1*^{KO} cells (Supplementary Fig. 5A).

Then, we tested whether olaparib could be used in combination with standard agents of CLL treatment such as the alkylating agent bendamustine or the BCR inhibitor ibrutinib, which could enhance olaparib cytotoxicity by synthetic lethality³⁰. In monotherapy, *SAMHD1*^{KO} cells were more sensitive to bendamustine (Fig. 3B), but not to ibrutinib (Supplementary Fig. 5B). Strikingly, combining bendamustine with olaparib resulted in synergistic effects in reducing cell survival of PGA1 cells (Combination Index–CI: *SAMHD1*^{WT} = 0.712; *SAMHD1*^{KO} = 0.751), being dual treatment more effective in *SAMHD1*^{KO} cells (Fig. 3B, Supplementary Fig. 5C). Furthermore, BCR inhibition with ibrutinib synergistically potentiated the effect of PARP inhibition (CI-*SAMHD1*^{WT} = 0.862; CI-*SAMHD1*^{KO} = 0.681), especially in *SAMHD1*^{KO} cells (Fig. 3C). Similarly, combining olaparib with ibrutinib increased induction of apoptosis particularly in *SAMHD1*^{KO} cells, demonstrated by a higher percentage of apoptotic cells (Fig. 3D, Supplementary Fig. 5D) and an enhanced PARP cleavage (Fig. 3E). Overall, these data indicate that olaparib, either in monotherapy or combined with other CLL treatments, effectively sensitizes *SAMHD1*^{KO}. Additionally, the reduced RAD51 localization in DSB lesions was consistent with an increase in sensitivity to the RAD51 inhibitor B02, as well as to the ATR inhibitor AZD6738 in *SAMHD1*^{KO} cells (Supplementary Fig. 5E).

***SAMHD1* mutations are infrequent but its dysfunction associates with dismal prognosis in CLL**

Finally, we evaluated the clinical impact of *SAMHD1* dysfunction through NGS analysis in 487 CLL patients. We identified 12 *SAMHD1* mutations in 8 cases (1.64%). These mutations included 3 nonsense and 9 missense substitutions that were predicted *in silico* as damaging for *SAMHD1* protein (Fig. 4A, Supplementary Table 6). All variants were present at high variant allele frequencies (VAF) (30–55%), suggesting its clonal nature. Moreover, *SAMHD1* mutated (*SAMHD1*^{MUT}) patients harbored other high-risk genetic alterations such as *TP53* or *ATM* mutations or losses (Supplementary Table 6).

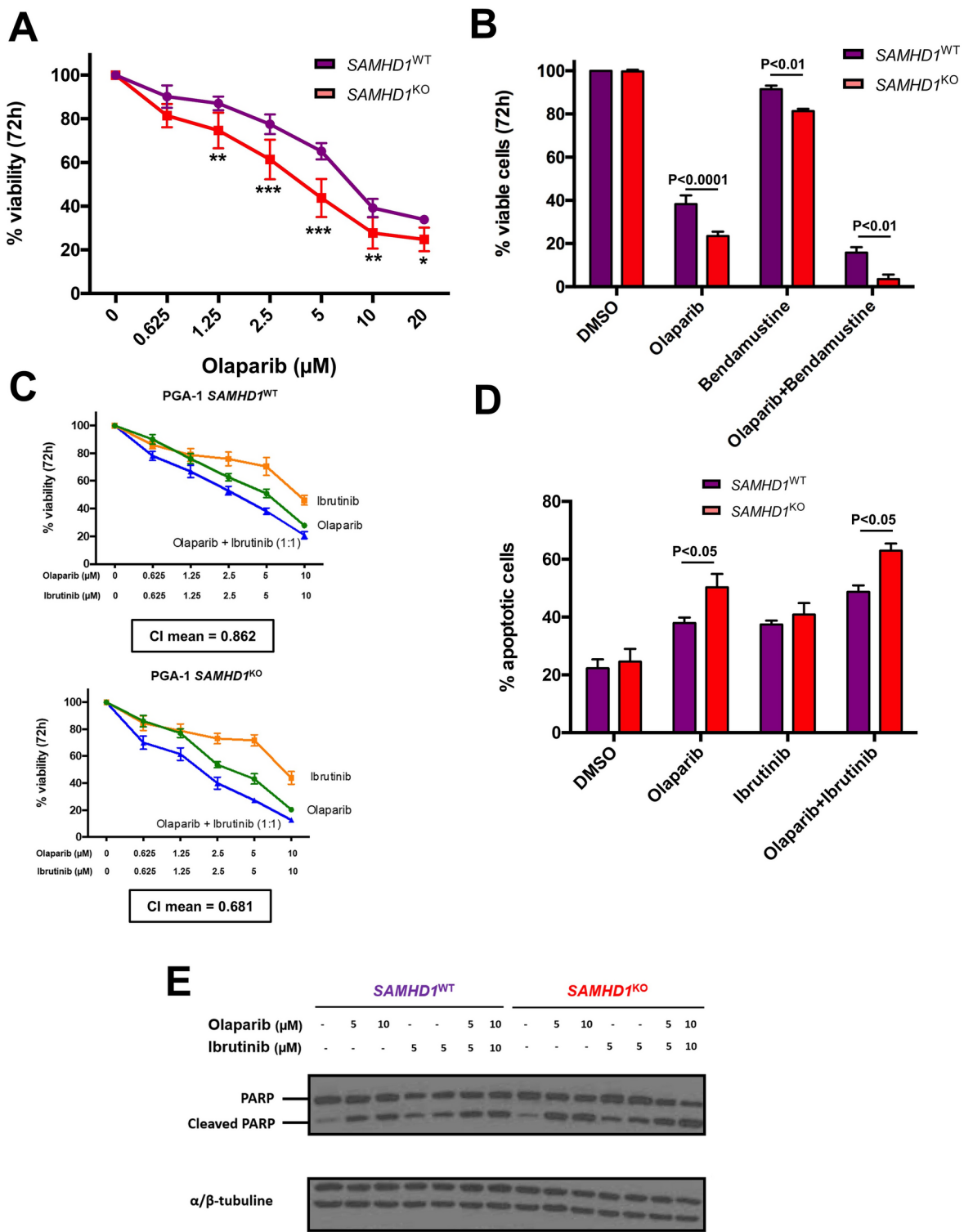
In additional CLL cohorts, the frequency of *SAMHD1* mutations varied depending on the patient population. In the largest cohort of pre-treatment patients analyzed (n = 1,009), the frequency was 1.5%³, while a separate study of treatment-naïve patients (n = 200) reported a slightly higher frequency of 3%¹⁴. Interestingly, *SAMHD1* variants were more prevalent among relapsed/refractory patients who had received immunochemotherapy, reaching 11% in a smaller cohort (n = 63)¹⁴. This elevated frequency was consistent with findings from another relapsed/refractory cohort, where the mutation rate was 9.6% (n = 114)¹⁵. Across these studies, 43 *SAMHD1* mutations were reported in 40 CLL patients^{3,14,15} (Supplementary Table 7). 75% (36/48) of these mutations were missense, being most of them (~80%, 29/36) annotated by bioinformatic predictors as likely pathogenic. In addition, 7 nonsense variations and 5 frameshift mutations were detected. The mutations were broadly distributed throughout the protein structure, affecting functional domains, allosteric and catalytic sites (Fig. 4A). The median VAF was 59.3% (range 8.15%–99.65%), with over 90% having a VAF > 25%, suggesting that these variants were mainly clonal, as previously reported¹⁴ (Supplementary Table 7).

Extending our investigations to the CLL-map project³, *SAMHD1*^{MUT} CLL cases (n = 15) had significantly shorter failure free-survival (FFS) compared to *SAMHD1*^{WT} patients (n = 994) (median 46 vs 57 months; p = 0.033) (Fig. 4B). Moreover, *SAMHD1*^{MUT} patients exhibited a trend towards reduction of time to first treatment (TFT) (median 32 vs 67 months; p = 0.069) (Supplementary Fig. 6A). Stratifying CLL patients from two independent cohorts based on *SAMHD1* expression levels, CLL cases with low *SAMHD1* expression associated with shorter TFT (median 47 vs 77 months; p = 0.00073) and overall survival (OS) (median 154 months vs not reached; p = 0.0046) compared to those with high *SAMHD1* expression in the CLL-map portal (Fig. 4C). These findings were independently validated in the GSE22762 dataset, in which low *SAMHD1* expression was similarly correlated with reduced TFT and OS (Supplementary Fig. 6B and C). Thus, both loss-of-function mutations and reduced expression of *SAMHD1* are implicated in adverse prognosis of CLL patients.

Discussion

Despite significant advances from large-scale sequencing studies over the last years^{3,5,18,19}, little is known about the biological and prognostic impact of most putative drivers in CLL such as *SAMHD1*. Our work provides a comprehensive analysis of the biological impact of *SAMHD1* dysfunction in CLL disease. Using novel CRISPR/Cas9-edited CLL cellular models, we show that loss of *SAMHD1* negatively affects the DDR and makes CLL cells hypersensitive to therapeutic approaches based on PARP inhibitors. Moreover, our results reinforce that not only mutations, but also altered gene expression of *SAMHD1*, are clinically relevant in CLL. Thus, our data underscore *SAMHD1* alterations as a possible biomarker of worse prognosis in CLL¹⁴, as it has been previously proposed in other solid tumors such as colon cancer^{22,37}.

Our findings uncover that *SAMHD1* dysfunction reduced HR efficiency in the context of CLL disease. Similarly, Daddacha *et al.* observed that *SAMHD1* localizes at DSBs in response to DNA damage to facilitate HR by promoting RAD51 recruitment¹¹. In our study, we demonstrate that *SAMHD1* depletion not only impairs RAD51 recruitment but also disrupts BRCA1 recruitment to DSBs. Furthermore, we confirm the colocalization of *SAMHD1* with the HR marker BRCA1 at DNA damage foci. This observation aligns with a previous study that identified the colocalization of *SAMHD1* with 53BP1, another DDR-related protein¹⁴. Additionally, through transcriptomic analysis of CLL patient data, we reveal a significant linear correlation between *SAMHD1* and

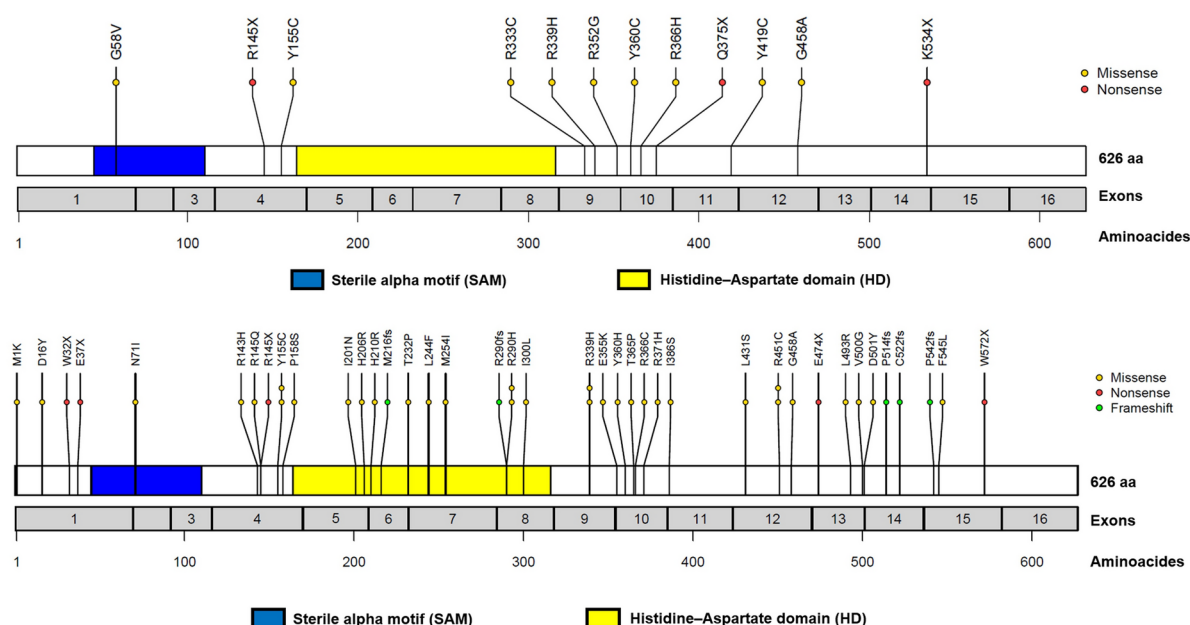


BRCA1 expression in CLL patients, providing further evidence of their functional relationship. Overall, our results substantiate a novel mechanistic role for SAMHD1 in enabling efficient BRCA1-mediated repair, as initially described in solid tumor models¹¹. Beyond this impact on HR, SAMHD1 deficiency compromises DDR signaling as SAMHD1 loss impairs cell cycle arrest in G2/M phase in response to DNA damage. We hypothesize that the moderate overexpression of p-Chk2 in SAMHD1^{KO} cells relative to SAMHD1^{WT} could enhance cell cycle arrest in G1 phase^{22–24}. This hypothesis aligns with previous studies reporting that defects in dNTPase function caused by SAMHD1 deficiency may lead to a G1 arrest^{8,17,25} and genomic instability²⁶. Taken together, our findings propose SAMHD1 as a critical mediator of HR and DDR integrity, offering new insights into its role in genomic stability.

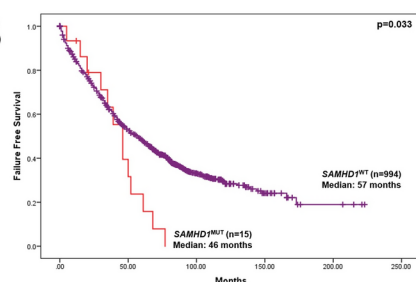
Our work provides evidence of hypersensitivity to olaparib in SAMHD1^{KO} cells. PARP inhibition is an approved treatment for HR-deficient solid tumors³⁴ and a potential therapeutic approach for hematological

Fig. 3. Response of *SAMHD1*^{KO} cells to olaparib in monotherapy and combined with bendamustine/ ibrutinib. (A) Cell viability studies by MTT assay in response to increasing doses of olaparib (0.625–20 μ M) for 72 h. Percentage of live cells is expressed relative to DMSO control. Differences between PGA-1 *SAMHD1*^{WT} and *SAMHD1*^{KO} clones are summarized by asterisks. Data are summarized as the mean \pm SD of three independent experiments. (B) Drug response to olaparib (20 μ M), bendamustine (20 μ M) and combination of both drugs (ratio 1:1) in PGA-1 *SAMHD1*^{WT} and *SAMHD1*^{KO} by measuring cell viability with MTT assay after 72 h. Data are summarized as the mean \pm SD of three independent experiments. (C) Dose–response curve of viable cells (%; relativized to untreated cells) after treatment with olaparib, ibrutinib and their combination at a 1:1 ratio. Data are presented as the mean \pm SD of three independent experiments. Combination index (CI) was calculated using Calcsyn. (D) Determination of cytotoxicity after 48-h treatment with olaparib (7.5 μ M), ibrutinib (7.5 μ M) and the combination of these drugs (1:1) in PGA-1 cells by measuring the percentage of apoptotic cells (annexin V + / PI+) with annexin V/PI staining. Data are presented as the mean \pm SD of three independent experiments. (E) Western blot analyses reflecting PARP cleavage as an apoptosis marker after treatment with olaparib, ibrutinib and their combination (ratio 1:1).

A



B



C

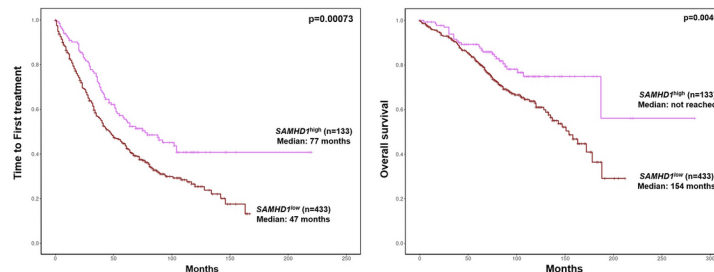


Fig. 4. Clinical impact of *SAMHD1* dysfunction in CLL patients. (A) Diagrammatic representation illustrating the distribution of *SAMHD1* mutations identified in CLL patients from the local cohort (up) and those previously reported in three CLL cohorts (down)^{3,14,15}. These variants are represented according to the amino acid change at the protein level (Transcript: ENST00000262878). Each circle represents a *SAMHD1* mutation, and its color means the type of mutation (missense, nonsense or frameshift). (B) Kaplan–Meier curve of failure free survival analysis of *SAMHD1* mutated (*SAMHD1*^{MUT}, red line) vs *SAMHD1* non-mutated (*SAMHD1*^{WT}, purple line) CLL patients from the CLL-map portal³. (C) Kaplan–Meier plots showing the association between *SAMHD1* expression and the time to first treatment (left) and overall survival (right) in CLL from the CLL-map portal³. CLL patient were grouped according to *SAMHD1* expression levels: low (dark red line) and high (light purple line).

malignancies^{16,28}, especially in CLL cells with DDR-related gene mutations^{20,30}. Furthermore, bendamustine or ibrutinib synergistically enhance olaparib sensitivity in CLL cells, mainly in the context of *SAMHD1*^{KO}, similar to previous observations in *ATM*-deficient CLL cells^{30,38}. These findings suggest that PARP inhibition could be a therapeutic strategy to use in CLL cells with defective DDR. In addition, previous research have demonstrated that ibrutinib produced a HR-impairment through RAD51 dysregulation which could explain the synergy effects of this drug with olaparib in *SAMHD1*^{KO} cells³⁰.

Moreover, we showed that *SAMHD1*^{KO} increases efficacy of fludarabine in CLL cells. Previous studies have identified that *SAMHD1* influences the response to nucleoside analogues²¹. Moreover, in various hematological malignancies, depletion of *SAMHD1* increases the cytarabine cytotoxicity, showing better chemotherapy responses in those patients with low *SAMHD1* expression^{39–42}. However, this observation is contradictory with the higher *SAMHD1* mutational frequency observed in relapsed/refractory to chemotherapy CLL cohorts. The presence of high-risk genetic alterations in relapsed CLL cases, even when *SAMHD1* is mutated, may contribute to poorer chemotherapy responses^{14,15}. In fact, *SAMHD1*^{MUT} CLL patients of the sequenced cohort harbored other high-risk alterations. In this way, *SAMHD1*^{KO} cells could be selected after fludarabine-based treatment, generating a non-death cellular pool with higher genomic instability that could increase relapse risk. In addition, DNA damaging agents such as fludarabine, bendamustine or etoposide further potentiate DNA repair defects and increase apoptosis in *SAMHD1*^{KO} cells, reinforcing the vulnerability of cells with *SAMHD1* mutations to DNA damage inducers¹¹.

Our findings on the biological impact of *SAMHD1* mutations highlights the importance of *SAMHD1* in the cellular response to DNA damage to ensure genomic stability. We could hypothesize that the defective DNA damage repair likely influences clinical outcomes, with *SAMHD1* dysfunction in CLL patients associating with unfavorable prognosis. Considering the molecular features of CLL, the identification of *SAMHD1* as a valuable prognostic marker contributes to our understanding of the molecular landscape of this disease and set the basis to the development of successful individual therapies. Moreover, our results emphasize the important role of DNA damage repair in CLL pathogenesis, as mutations in *TP53* and *ATM* occur frequently in CLL patients, underscoring this pathway as a promising therapeutic target.

In conclusion, our results provide evidence of the significance of *SAMHD1* mutations in the cellular response to DNA damage and uncover *SAMHD1* as a potential prognostic marker with clinical relevance. We propose that PARP inhibition in monotherapy or combined with DNA damage inducers or BTK inhibitors could be promising options for treatment of CLL patients with *SAMHD1* alterations. Thus, this study contributes to gain insight into the heterogeneous landscape of CLL mutations and propose promising therapeutic approaches for a subgroup of high-risk CLL patients.

Methods

Generation of *SAMHD1*^{KO} CLL cell lines

The human CLL-derived cell lines PGA1, HG3 and MEC1 were used. *SAMHD1* mutational status was analyzed with a custom NGS panel. *SAMHD1* wild-type PGA1 and MEC1 cell lines were selected for CRISPR/Cas9 experiments (Supplementary Table 1).

PGA1 and MEC1 Cas9-expressing cell lines were previously established³⁶ and tested for Cas9 activity⁴³. To generate CLL cells knockout for *SAMHD1* (*SAMHD1*^{KO}), single-guide RNAs (sgRNAs) targeting *SAMHD1* (exon 4) were designed using CRISPick⁴⁴, prioritizing those with high on-target efficiency and low off-target effects (Supplementary Table 2). A non-targeting sgRNA served as a negative control (5'-ACGGAGGCTAA GCGTCGCAA-3'). SgRNAs were cloned into the pLKO5.sgRNA.EFS.tRFP plasmid (Addgene #57823)²⁷ and nucleofected into PGA1-Cas9 and MEC1-Cas9 using Amaxa Nucleofector II (Lonza, program X-005). 72 h post-transfection, mCherry+ cells were single-cell sorted using a FACSaria II cytometer (BD Biosciences) and clones were expanded and screened for the presence of *SAMHD1* truncating mutations (Supplementary Fig. 1A and 1B). Three *SAMHD1* loss-of-function clones were selected for functional studies.

Patients

The study involved 487 CLL patients diagnosed according to the International Workshop on CLL (iwCLL) criteria^{45,46}. Samples and clinical data from 16 Spanish institutions were centrally analyzed at the Molecular Cytogenetics Unit of the Cancer Research Center in Salamanca, Spain (Supplementary Table 3). This study was approved by the ethics committee of Hospital Universitario de Salamanca (Comité Ético de Investigación Clínica, Hospital Universitario de Salamanca). Written informed consent was obtained from all participants before they entered the study in accordance to the Declaration of Helsinki. CLL samples were analyzed before first-line treatment. Additional clinical information was obtained from three previously documented CLL cohorts^{3,14,15} and the CLL-map portal³.

Next generation sequencing (NGS)

NGS analyses were performed in 487 CLL patients. Genomic DNA of CD19+ B-lymphocytes was isolated from peripheral blood or bone marrow by magnetically activated cell sorting (B-cell purity > 98%)^{29–32}. Libraries of exonic regions from 54 CLL-associated genes were prepared using the Agilent SureSelect^{QXT} Target Enrichment system for Illumina Multiplexed Sequencing (Agilent Technologies) (Supplementary Table 4). Paired-end sequencing (151-bp reads) was conducted on an Illumina NextSeq instrument (see Supplementary methods).

Bioinformatic analyses

The clinical implications of *SAMHD1* mutations in CLL were assessed in 1,009 patients from the CLLmap portal³. The impact of low *SAMHD1* expression was evaluated in two transcriptomic data sets, one with 566³ and another with 107 CLL cases³³. Time to first treatment (TFT), overall survival (OS) and failure free survival

(FFS) were estimated by the Kaplan–Meier method, with group comparisons performed using the log-rank test. Overrepresented biological processes associated with *SAMHD1* dysfunction were identified using a Pearson correlation-based approach, focusing on genes with a Pearson Correlation coefficient $|R\text{-squared}| > 0.3$ and adjusted $p\text{-value} < 0.05$. Gene enrichment and functional annotation analyses were conducted using DAVID, focusing on gene ontology (GO) at biological process (BP) level (see supplementary methods).

Statistical approach

Statistical analyses were performed with GraphPad Prism v6. Data are represented as mean \pm standard deviation (SD). Student's t test, Mann–Whitney and ANOVA were used to determine statistical significance. $P\text{-values} < 0.05$ were considered statistically significant. Experiments were performed in 3 independent *SAMHD1*^{WT} and *SAMHD1*^{KO} clones.

Data availability

All data and information concerning this study will be made available from the corresponding authors (jmhr@usal.es and mariahs@ucm.es) upon reasonable request.

Received: 2 October 2024; Accepted: 7 March 2025

Published online: 26 March 2025

References

- Gaidano, G., Foà, R. & Dalla-Favera, R. Molecular pathogenesis of chronic lymphocytic leukemia. *J. Clin. Investig.* **122**(10), 3432–3438 (2012).
- Zenz, T., Mertens, D., Küppers, R., Döhner, H. & Stilgenbauer, S. From pathogenesis to treatment of chronic lymphocytic leukaemia. *Nat. Rev. Cancer* **10**(1), 37–50 (2010).
- Knisbacher, B. A. et al. Molecular map of chronic lymphocytic leukemia and its impact on outcome. *Nat. Genet.* **54**(11), 1664–1674 (2022).
- Puente, X. S. et al. Non-coding recurrent mutations in chronic lymphocytic leukaemia. *Nature* **526**(7574), 519–524 (2015).
- Landau, D. A. et al. Mutations driving CLL and their evolution in progression and relapse. *Nature* **526**(7574), 525–530 (2015).
- Goldstone, D. C. et al. HIV-1 restriction factor SAMHD1 is a deoxynucleoside triphosphate triphosphohydrolase. *Nature* **480**(7377), 379–382 (2011).
- Powell, R. D., Holland, P. J., Hollis, T. & Perrino, F. W. Aicardi-Goutières syndrome gene and HIV-1 restriction factor SAMHD1 is a dGTP-regulated deoxynucleotide triphosphohydrolase. *J. Biol. Chem.* **286**(51), 43596–43600 (2011).
- Franzolin, E. et al. The deoxynucleotide triphosphohydrolase SAMHD1 is a major regulator of DNA precursor pools in mammalian cells. *Proc. Natl. Acad. Sci. U. S. A.* **110**(35), 14272–14277 (2013).
- Mathews, C. K. Deoxyribonucleotide metabolism, mutagenesis and cancer. *Nat. Rev. Cancer* **15**(9), 528–539 (2015).
- Rentoft, M. et al. Heterozygous colon cancer-associated mutations of SAMHD1 have functional significance. *Proc. Natl. Acad. Sci. U. S. A.* **113**(17), 4723–4728 (2016).
- Daddacha, W. et al. SAMHD1 promotes DNA end resection to facilitate DNA repair by homologous recombination. *Cell Rep.* **20**(8), 1921–1935 (2017).
- Rice, G. I. et al. Mutations involved in Aicardi-Goutières syndrome implicate SAMHD1 as regulator of the innate immune response. *Nat. Genet.* **41**(7), 829–832 (2009).
- Crow, Y. J. & Rehwinkel, J. Aicardi-Goutières syndrome and related phenotypes: Linking nucleic acid metabolism with autoimmunity. *Hum. Mol. Genet.* **18**(R2), 130–136 (2009).
- Clifford, R. et al. SAMHD1 is mutated recurrently in chronic lymphocytic leukemia and is involved in response to DNA damage. *Blood* **123**(7), 1021–1031 (2014).
- Guiéze, R. et al. Presence of multiple recurrent mutations confers poor trial outcome of relapsed/refractory CLL. *Blood* **126**(18), 2110–2117 (2015).
- Fong, P. C. et al. Inhibition of Poly(ADP-Ribose) Polymerase in Tumors from BRCA Mutation Carriers. *N. Engl. J. Med.* **361**(2), 123–134 (2009).
- Coggins, S. A., Mahboubi, B., Schinazi, R. F. & Kim, B. SAMHD1 functions and human diseases. *Viruses* **12**(4), 1–28 (2020).
- Quesada, V. et al. Exome sequencing identifies recurrent mutations of the splicing factor SF3B1 gene in chronic lymphocytic leukemia. *Nat. Genet.* **44**(1), 47–52 (2012).
- Puente, X. S. et al. Whole-genome sequencing identifies recurrent mutations in chronic lymphocytic leukaemia. *Nature* **475**(7354), 101–105 (2011).
- Knecht, K. M. et al. The structural basis for cancer drug interactions with the catalytic and allosteric sites of SAMHD1. *Proc. Natl. Acad. Sci. U. S. A.* **115**(43), E10022–E10031 (2018).
- Schneider, C. et al. SAMHD1 is a biomarker for cytarabine response and a therapeutic target in acute myeloid leukemia. *Nat. Med.* **23**(2), 250–255 (2017).
- Zhang, Z. et al. Involvement of SAMHD1 in dNTP homeostasis and the maintenance of genomic integrity and oncotherapy (Review). *Int. J. Oncol.* **56**(4), 879–888 (2020).
- Zannini, L., Delia, D. & Buscemi, G. CHK2 kinase in the DNA damage response and beyond. *J. Mol. Cell Biol.* **6**(6), 442–457 (2014).
- Maréchal, A. & Zou, L. DNA damage sensing by the ATM and ATR kinases. *Cold Spring Harb. Perspect. Biol.* **5**(9), 1–18 (2013).
- Bonifati, S. et al. SAMHD1 controls cell cycle status, apoptosis and HIV-1 infection in monocytic THP-1 cells. *Virology* **495**, 92–100 (2016).
- Kretschmer, S. et al. SAMHD1 prevents autoimmunity by maintaining genome stability. *Ann. Rheum. Dis.* **74**(3), 1–8 (2015).
- García-Tuñón, I. et al. The CRISPR/Cas9 system efficiently reverts the tumorigenic ability of BCR/ABL in vitro and in a xenograft model of chronic myeloid leukemia. *Oncotarget* **8**(16), 26027–26040 (2017).
- Skelding, K. A. & Lincz, L. F. PARP inhibitors and haematological malignancies—Friend or foe?. *Cancers* **13**, 5328 (2021).
- Quijada-Álamo, M. et al. Dissecting the role of TP53 alterations in del(11q) chronic lymphocytic leukemia. *Clin. Transl. Med.* <https://doi.org/10.1002/ctm2.304> (2021).
- Quijada-Álamo, M. et al. Biological significance of monoallelic and biallelic BIRC3 loss in del(11q) chronic lymphocytic leukemia progression. *Blood Cancer J.* **11**(7), 1–11 (2021).
- Pérez-Carretero, C. et al. Chronic lymphocytic leukemia patients with IGH translocations are characterized by a distinct genetic landscape with prognostic implications. *Int. J. Cancer* **147**(10), 2780–2792 (2020).
- Pérez-Carretero, C. et al. TRAF3 alterations are frequent in del-3'IGH chronic lymphocytic leukemia patients and define a specific subgroup with adverse clinical features. *Am. J. Hematol.* **97**(7), 903–914 (2022).

33. Herold, T. et al. An eight-gene expression signature for the prediction of survival and time to treatment in chronic lymphocytic leukemia. *Leukemia* **25**(10), 1639–1645 (2011).
34. Paik, E. S., Chang, H. K. & Lee, S. Prevalence of homologous recombination deficiency in first-line PARP inhibitor maintenance clinical trials and further implication of personalized treatment in ovarian cancer. *Cancers (Basel)* **15**(12), 3095 (2023).
35. Helleday, T., Bryant, H. E. & Schultz, N. Poly(ADP-ribose) polymerase (PARP-1) in homologous recombination and as a target for cancer therapy. *Cell Cycle* **4**(9), 1176–1178 (2005).
36. Quijada-Álamo, M. et al. CRISPR/Cas9-generated models uncover therapeutic vulnerabilities of del(11q) CLL cells to dual BCR and PARP inhibition. *Leukemia* **34**(6), 1599–1612 (2020).
37. Park, K. et al. Aicardi-Goutières syndrome-associated gene SAMHD1 preserves genome integrity by preventing R-loop formation at transcription–replication conflict regions. *PLoS Genet.* **17**, 1–24 (2021).
38. Stankovic, T. & Skowronska, A. The role of ATM mutations and 11q deletions in disease progression in chronic lymphocytic leukemia. *Leuk. Lymphoma* **55**(6), 1227–1239 (2014).
39. Rassidakis, G. Z. et al. Low-level expression of SAMHD1 in acute myeloid leukemia (AML) blasts correlates with improved outcome upon consolidation chemotherapy with high-dose cytarabine-based regimens. *Blood Cancer J.* <https://doi.org/10.1038/s41408-018-0134-z> (2018).
40. Wang, T. et al. SAMHD1 mutations and expression in mantle cell lymphoma patients. *Front. Oncol.* **11**(December), 1–10 (2021).
41. Roeder, T. et al. The impact of SAMHD1 expression and mutation status in mantle cell lymphoma: An analysis of the MCL Younger and Elderly trial. *Int. J. Cancer* **148**(1), 150–160 (2021).
42. Xagoraris, I. et al. Expression of the novel tumour suppressor sterile alpha motif and HD domain-containing protein 1 is an independent adverse prognostic factor in classical Hodgkin lymphoma. *Br. J. Haematol.* **193**(3), 488–496 (2021).
43. Doench, J. G. et al. Rational design of highly active sgRNAs for CRISPR-Cas9-mediated gene inactivation. *Nat. Biotechnol.* **32**(12), 1262–1267 (2014).
44. CRISPick [Internet]. <https://portals.broadinstitute.org/gppx/crispick/public> (2023).
45. Swerdlow, S. H. et al. The 2016 revision of the World Health Organization classification of lymphoid neoplasms. *Blood* **127**(20), 2375–2390 (2016).
46. Hallek, M. Guidelines for the diagnosis and treatment of chronic lymphocytic leukemia: A report from the International Workshop on Chronic Lymphocytic Leukemia updating the National Cancer Institute Working Group 1996 guidelines (Blood (2008) (111)). *Blood* **112**(13), 5259 (2008).
47. SwimmerPlot GitHub public site [Internet]. <https://cclmap.org/viz/swimmer-plot/> (2023).

Acknowledgements

We thank Almudena Martín-Martín, Sara González, Irene Rodríguez, Teresa Prieto, M^a Ángeles Ramos, Filomena Corral, M^a Almudena Martín, Ana Díaz, Ana Simón, María del Pozo, Isabel M Isidro, Vanesa Gutiérrez, Sandra Pujante, M^a Ángeles Hernández, Sandra Santos and Cristina Miguel from the Cancer Research Center of Salamanca, Spain, for their technical support. We are grateful to Ángel Prieto and Ana I García from the Microscopy Unit and María Luz Sánchez from Cytometry Unit, from the Cancer Research Center of Salamanca for their technical assistance. We thank Javier Borrajo from the Service of NUCLEUS, University of Salamanca for his help with the irradiation experiments. We are deeply grateful to Teresa González, Julio Dávila-Valls, María Jesús Vidal-Manceño, Josefina Galende, José Antonio Queizán, Carlos Aguilar and José Ángel Hernández-Rivas for providing patient samples and clinical information. This study has been funded by Instituto de Salud Carlos III (ISCIII) through the project "PI21/00983" and co-funded by the European Union, by grants (RD12/0036/0069) from Red Temática de Investigación Cooperativa en Cáncer (RTICC), Centro de Investigación Biomédica en Red de Cáncer (CIBERONC CB16/12/00233), Residual disease assessment in hematologic malignancies to improve patient-relevant outcomes across Europe (RESOLVE, GA number 101136502), HORIZON-MISS-2023-CANCER-01-03 and grant PID2023-149241OA-I00 funded by MICIU/AEI/10.13039/501100011033 and by ERDF/EU. ARS is fully supported by predoctoral research fellowship 2022 from Junta de Castilla y León and cofinanced by the European Social Fund Plus (FSE+) (JCYL-EDU/1868/2022 PhD scholarship). CPC is supported by a research grant from FEHH ("Fundación Española de Hematología y Hemoterapia"; Beca de Investigación FEHH 2022).

Author contributions

ARS and MHS designed and performed the experiments, conducted data analysis and wrote the manuscript. MQA and CPC contributed to the design of the functional experiments, interpreted the results and critically reviewed the manuscript. ABH designed DNA damage repair experiments and interpreted the results. AAB contributed to bioinformatic data analysis. JDV, AR, AGC provided patient's clinical data. RBS and AERV designed sequencing studies and contributed to data analysis. JMHR conceived the study, supervised the research and critically reviewed and approved the final version of the manuscript. All authors discussed the results and revised the manuscript.

Declarations

Competing interests

The authors declare no competing interests.

Ethics declarations

This study was approved by the ethics committee of Hospital Universitario de Salamanca and written informed consent was obtained from all participants before they entered the study in accordance to the declaration of Helsinki.

Additional information

Supplementary Information The online version contains supplementary material available at <https://doi.org/10.1038/s41598-025-93629-7>.

Correspondence and requests for materials should be addressed to M.H.-S.

Reprints and permissions information is available at www.nature.com/reprints.

Publisher's note Springer Nature remains neutral with regard to jurisdictional claims in published maps and institutional affiliations.

Open Access This article is licensed under a Creative Commons Attribution-NonCommercial-NoDerivatives 4.0 International License, which permits any non-commercial use, sharing, distribution and reproduction in any medium or format, as long as you give appropriate credit to the original author(s) and the source, provide a link to the Creative Commons licence, and indicate if you modified the licensed material. You do not have permission under this licence to share adapted material derived from this article or parts of it. The images or other third party material in this article are included in the article's Creative Commons licence, unless indicated otherwise in a credit line to the material. If material is not included in the article's Creative Commons licence and your intended use is not permitted by statutory regulation or exceeds the permitted use, you will need to obtain permission directly from the copyright holder. To view a copy of this licence, visit <http://creativecommons.org/licenses/by-nc-nd/4.0/>.

© The Author(s) 2025